Rotor Noise Due to Atmospheric Turbulence Ingestion—Part II: Aeroacoustic Results

R. K. Amiet,* J. C. Simonich,† and R. H. Schlinker‡
United Technologies Research Center, East Hartford, Connecticut

A previously developed analysis for noise prediction due to turbulent inflow to a propeller or helicopter rotor has been extended to treat nonisotropic turbulence. The turbulence is calculated using a mean-flow contraction model combined with rapid distortion theory as described in the companion paper.[1] The noise model is based on an analysis for a flat plate in rectilinear motion through a turbulent field. By assuming that the rotor is in rectilinear motion at each instant of time, the overall spectrum is calculated by averaging the instantaneous spectrum over time. The mean-flow distortion stretches the turbulence, decreasing the velocities along the principal axis of the stretching (strain). When the principal axis of the stretching lies close to the rotor axis, the distortion acts to decrease the upwash velocities on the rotor and thus decreases the noise from that for isotropic turbulence. The correlation area in the plane of the rotor also is decreased tending to decrease the noise further. Conversely, if the principal stretching direction lies close to the rotor plane, an increase in the noise is possible. Acoustic energies at the observer location are calculated and compared to the energy of the turbulence as affected by the contraction.

Nomenclature

B	= blade number
C	= contraction ratio
c	= chord
c_0	= sound speed
F	= vector dipole strength
k	= reduced frequency
L	= turbulence integral scale
M	= Mach number
M_f	= flight (in plane) Mach number
M_n	= Mach number component in direction of observer
M_t	= rotor tip Mach number
M_z	= axial Mach number
p	= pressure
R_0	= rotor radius
r	= distance to far field
U_z	= axial velocity
V_t	= rotor tip velocity
$\overline{w^2}$	= mean square axial velocity fluctuation
x,y,z	= Cartesian coordinates with origin at rotor hub
δ_{ij}	= Kronecker delta function
ϵ_{ij}	= Eulerian strain tensor
η_{ij}	= Lagrangian strain tensor
θ	= angle of observer from rotor axis
μ_1,μ_2,μ_3	= energy of turbulence in three directions
τ	= airfoil thickness

Received Sept. 16, 1986; revision received May 27, 1989.

*Senior Research Engineer, Aeroacoustics and Gas Dynamics Research. Member AIAA.

†Research Engineer, Aeroacoustics and Gas Dynamics Research. Member AIAA.

‡Supervisor, Aeroacoustics and Gas Dynamics Research. Member AIAA.

Introduction

A HELICOPTER rotor moving through a turbulent flowfield experiences fluctuating forces due to the random upwash seen by the rotor. These time-dependent forces are a source of broadband noise.

Previous analytical methods developed to predict this noise considered isotropic turbulence rotor inflows only. Although a generalized acoustic analysis existed, realistic turbulence conditions at the rotor face, needed as inputs to the analysis, were unknown. One mechanism that influenced the turbulent flowfield was the mean-flow contraction. As noted by Hanson,[2] the stretching of the turbulence by the inflow could be a significant factor in the noise generated.

A previous analysis[3] calculated the noise produced by this stretching in a somewhat ad hoc manner. By inputting a decreased axial flow into the rotor noise prediction program, it was possible to simulate the eddy stretching and the resulting multiple eddy chopping. This in turn leads to the enhancement of narrowband random tones. Results calculated by this method, however, have the same acoustic energy as with no stretching. Also, the method does not take into consideration the changes in the energy of the various velocity components produced by the stretching nor does it consider the change in length scale in the rotor plane.

The objective of the present study is to define the atmospheric turbulence field by using rapid distortion theory. This is then used as input to a previously developed first principles turbulence ingestion noise theory. The resulting calculations are then compared with expectations based on energy considerations. Since rapid distortion theory neglects the tendency for nonisotropic turbulence to revert back to the isotropic state, the present predictions may somewhat overestimate the effect produced by an actual distortion, but further investigation of this point is needed.

The present method, using a calculated nonisotropic turbulence, will give a prediction of the acoustic energy produced by isotropic turbulence. One should use care when examining the figures not to identify a change in the peak level of a blade passage harmonic with a change in the acoustic energy. Depending on the axial extent of a turbulent eddy, the width of

the peak will vary significantly; the peak level of two harmonics can differ even though they have the same value of acoustic energy.

Previous Investigations

The study of the noise produced by interaction of turbulence with an airfoil has been an ongoing research area for many years. The following summary is not intended to be a comprehensive review but only to touch the primary developments as they relate to the objectives of the present program. For an extensive historical development in this topic area the reader is referred to the review papers of George[4] or Brooks and Schlinker.[5]

Sharland[6] was one of the first to demonstrate the noise generated by the interaction of an airfoil with a turbulent flow. He placed a small isolated flat plate in a nozzle exhaust and obtained good agreement between the experimental results and a simple theory based on the concept of unsteady surface pressure correlation area. Dean[7] improved on these experiments by measuring the airfoil surface pressure at a point and the spectrum of the vertical component of turbulence, in addition to the far-field noise. Approximate calculations were made of the airfoil surface pressure correlation lengths.

Approaches such as these, based on a surface pressure correlation area, present the difficult task of determining the correlation area as a prerequisite to the noise prediction. The alternative approach used here is to formulate the prediction method in terms of the inflow turbulence spectrum together with a general solution for the airfoil response functions for skewed gusts and nonzero Mach number. To be complete, such a prediction must include noncompactness effects of the airfoil surface pressure.

Prediction methods based on airfoil response functions have been introduced by several authors.[8-16] However, many of these are limited in some respect. For example, Refs. 8 and 9 use low-frequency airfoil response functions appropriate to incompressible flow. This leads to incorrect high-frequency behavior since the Sears function (incompressible flow) decays as $k^{-1/2}$, whereas the correct behavior for compressible flow is k^{-1}. Thus, these prediction methods significantly overpredict the high-frequency spectrum when the acoustic wavelength is comparable to or smaller than the chord. Also, the predictions in Refs. 8 and 9 assume chordwise compactness of the surface pressure, which is significantly in error at the higher frequencies.

The prediction method of Amiet[10] was one of the first to incorporate all of the above factors into a consistent acoustic model. The procedure was based on accurate airfoil response functions for nonzero Mach number. Noncompactness effects of the airfoil surface pressure source term in both the chordwise and spanwise directions were included. Comparison with the experiment by Paterson and Amiet[11] showed good agreement.

The preceding noise prediction methods are limited to the case of rectilinear airfoil motion through turbulence. The case of a rotating airfoil interacting with turbulence, such as a propeller or helicopter rotor in hover, was considered by Homicz and George.[12] This analysis made use of the exact expression for the pressure field of a rotating dipole. However, approximations were needed to include the effects of spanwise correlation length and the assumption of chordwise compactness of the surface pressure was used. Also, the airfoil response function was a low-frequency approximation, which has inaccuracies at high frequency.

Amiet[13] formulated a different approach to modeling the rotating blade case. Rather than use the expression for a rotating dipole, the rectilinear motion analysis[10] was used to calculate the instantaneous spectrum of the rotor as a function of azimuthal position. Whereas this appears to be an approximation, it becomes an exact analysis for high frequency and gives good results for frequencies approaching the rotor frequency. The flat plate airfoil response functions used are accurate over the entire frequency range and the effects of both chordwise and spanwise noncompactness are included. A major advantage of this approach is that it can be readily generalized to the case of helicopter forward flight.

George and Chow[14] compared the method of Amiet with that of George and Kim.[15] The method of George and Kim was obtained from that of Homicz and George[12] using a high-frequency approximation. Comparison of the methods of Amiet and George and Kim with available data showed comparable results for the two methods.

Comparisons between theory and experiment were made by Paterson and Amiet.[11] One extension made to the theory for these comparisons was to simulate the effect of eddy elongation by varying the drift velocity of the eddy through the rotor disk during forward flight. For low-drift velocities, a given eddy would be cut by the rotor more often than for high-drift velocities. Assuming the rotor tip velocity is significantly greater than the drift velocity, lowering the drift velocity does not change the overall acoustic energy, but lowering does narrow the peak widths and increase the heights of the harmonics of blade passage frequency.

The present study extends this analysis by performing a more rigorous calculation of the sound produced by a stretched eddy. By combining a mean-flow contraction calculation with a rapid-distortion calculation for the turbulence, the present treatment allows for distortion of the turbulence spectrum. The distortion leads to a different result for the acoustic energy, in contrast to the above method of altering the eddy drift velocity, which results in the same acoustic energy.

Rotor Acoustic Model for Isotropic Turbulence

The model used for the acoustic calculations is basically unchanged from that described previously.[3,13] This previous analysis is described briefly below. The analysis begins with the result for the noise generated by a flat-plate airfoil in a turbulent stream.[10] This model assumes a flat-plate airfoil with a span significantly greater than the acoustic wavelength. The representation of the turbulence can be completely general and need not be isotropic. If flat-plate airfoil theories are to apply, the noise must be produced by eddies large compared to the actual airfoil thickness. If the airfoil thickness is denoted by τ, this gives an upper limit on the calculated frequency of U/τ where U is the freestream velocity.

This result for a flat-plate airfoil in rectilinear motion through turbulence is then generalized to the rotor case by simply averaging the spectrum over time. That is, the spectrum is treated as an "instantaneous spectrum," and an average is taken as the rotor moves around the azimuth to find the overall spectrum. This should be an accurate model so long as the rotor directivity does not change significantly in the time taken by the rotor to intersect an eddy; the model requires that the turbulence be small compared to the rotor diameter. The rationale for this approach is illustrated in Eq. (1). This is an expression derived by Lowson[16] for the far-field pressure of a dipole in accelerated motion. The first term is that for a dipole in rectilinear motion, and the second addresses the effects of acceleration. It can be seen that the second term is small compared to the first if the acoustic frequency of interest is significantly larger than the rotation frequency. The square brackets imply the expression is to be evaluated at the retarded time.

$$p = \left[\frac{1}{4\pi c_0 r^2(1-M_n)^2}\boldsymbol{x}\cdot\left(\dot{\boldsymbol{F}}+\frac{\boldsymbol{F}\dot{M}_n}{1-M_n}\right)\right] \qquad (1)$$

The geometry of the rotor is shown in Fig. 1.

Again, the turbulence need not be isotropic, in principle, but in practice it was more convenient to make the assumption of isotropic turbulence. This was both for convenience and because there was no model available for nonisotropic turbulence.

The airfoil response functions used include the effects of compressibility. Also, noncompactness effects of the blade

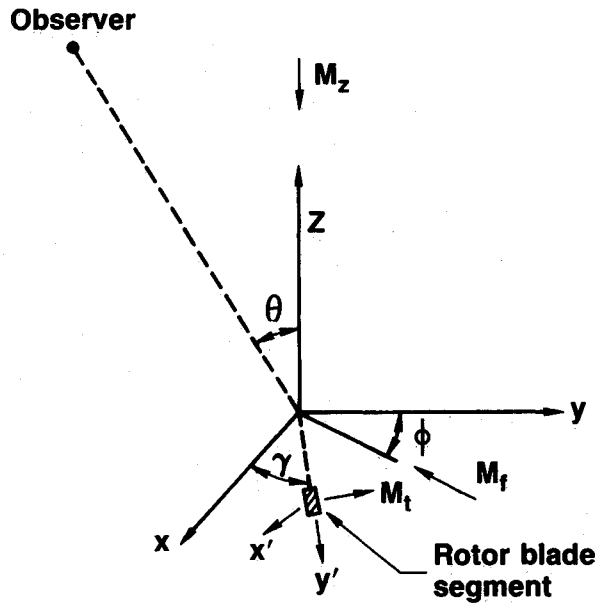

Fig. 1 Geometry of rotor model.

forces are included. These two effects, noncompactness and compressibility, are interrelated, and to include one without the other would be unsatisfactory.

Present Model

The model described previously was extended by including the effects of a distorted turbulence in the input. As described in the companion paper,[1] hereafter referred to as Part 1, rapid distortion theory[17,18] was used in conjunction with a model for the mean-flow contraction to calculate the spectrum of the turbulence. A more complete presentation of this rapid distortion analysis is given in Ref. 19. The turbulence spectrum prior to the distortion is assumed to be isotropic. After removing the convenient assumptions of isotropic turbulence in the program, the expression for the nonisotropic turbulence spectrum was introduced into the acoustic program.

A turbulence contraction works to increase the vorticity along the axis of the contraction and to decrease it in the two normal directions. This changes the energy of the velocity perturbations as shown in Fig. 2 from Ref. 18. This shows the relative change in the energy of the velocity perturbations in the axial direction and in the two normal directions for an isotropic turbulence having undergone a contraction. For this particular figure, it is assumed that the contraction is equal in the two directions normal to the contraction. The figure clearly shows the attenuation of the energy in the axial direction and the increase of energy in the two transverse directions. This results because the increase of the vorticity in the axial direction induced by the distortion produces greater velocity perturbations in the two transverse directions. The vorticity in the two normal directions is attenuated leading to a decrease in the energy of the velocity perturbations along the axis. This reasoning will be important later in explaining the calculated acoustic results.

The program used to calculate the results presented in this paper includes a correction to an error; this error produced incorrect results in a previous report.[20] The error occurred only in the calculations for the cases with nonisotropic turbulence; thus, previous calculations for the case of isotropic turbulence are correct. This correction can be significant (of the order of 10 dB depending on the case). It brings the acoustic results more into line with expectations given the preceding arguments concerning the energy of the velocity perturbations. (Recall that the acoustic energy is produced by the interaction of the velocity perturbations with the rotor blade.)

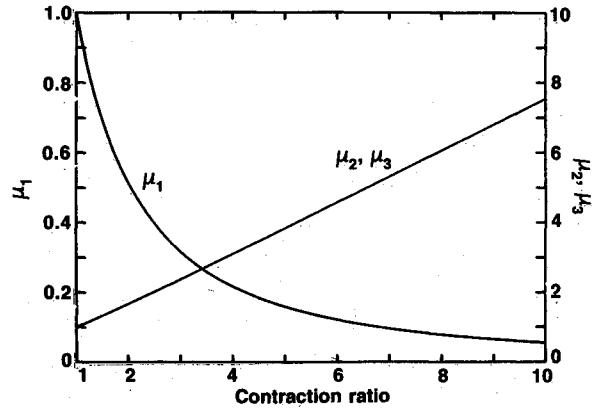

Fig. 2 Energy of velocity fluctuations in each of three directions after contraction; from Ref. 18.

Finite-Deformation Theory

The deformation tensor that is calculated in Part 1 of this analysis and used as input to the present acoustic program is specified in an absolute reference frame. For purposes of interpretation, it is useful to express this in terms of the principal strains since this gives a more physical representation of the strains. In fact, the analysis performed in Refs. 1, 19, and 20 for turbulence undergoing a rapid distortion could have been performed by the alternate technique of combining a rotation to the principal strain direction together with the analysis of Ribner and Tucker,[17] which was derived assuming a diagonal strain matrix, i.e., a strain matrix expressed in the form of principal strains.

Finite-strain theory must be used since a fluid can be distorted to any degree in contrast to the case of a solid deformation for which the theory of infinitesimal strains can usually be applied. This leads to the distinction between the Lagrangian strain tensor and the Eulerian strain tensor, which for infinitesimal strains are the same. Paraphrasing Love,[21] if a sphere is drawn in the fluid before the deformation, the sphere becomes an ellipsoid after the deformation; this is called the strain ellipsoid. Also, a particular ellipsoid before the deformation which becomes a sphere after the deformation is called the reciprocal strain ellipsoid. The principal axes of the reciprocal strain ellipsoid are called the principal axes of the strain.

If a_i are the coordinates of a particle before the deformation and x_j are the coordinates of the same particle after the deformation, the components of the Lagrangian strain tensor η_{ij} can be written[22]

$$\eta_{ij} = \frac{1}{2}\left(\frac{\partial x_s}{\partial a_i}\frac{\partial x_s}{\partial a_j} - \delta_{ij}\right) \tag{2}$$

The Eulerian strain tensor ϵ_{ij} has components

$$\epsilon_{ij} = \frac{1}{2}\left(\delta_{ij} - \frac{\partial a_s}{\partial x_i}\frac{\partial a_s}{\partial x_j}\right) \tag{3}$$

The three λ roots of the determinantal equation $|\eta_{ij} - \lambda\delta_{ij}| = 0$ are the values of the nonvanishing components of the reciprocal strain tensor in a coordinate system aligned with the principal axes and similarly for the strain tensor ϵ_{ij}. If the distance between any two particles before the deformation is represented by ds_0 and after the deformation by ds, then

$$ds^2 - ds_0^2 = 2\eta_{ij}da_ida_j \tag{4a}$$

$$ds^2 - ds_0^2 = 2\epsilon_{ij}dx_idx_j \tag{4b}$$

Thus, if the three principal reciprocal strains are η_1, η_2, η_3, the relative extensions are $(ds/ds_0)_i^2 = (1 + 2\eta_{ij})$, where i takes one of the values 1, 2, or 3 representing the three principal

directions. This can also be written in terms of ϵ_{ij} as $(ds_0/ds)_i^2 = 1 - 2\epsilon_{ii}$.

The convention used to represent the tensor $\partial x_i/\partial a_j$ in matrix form is

$$\partial x_i/\partial a_j = \begin{bmatrix} \partial x_1/\partial a_1 & \partial x_1/\partial a_2 & \partial x_1/\partial a_3 \\ \partial x_2/\partial a_1 & \partial x_2/\partial a_2 & \partial x_2/\partial a_3 \\ \partial x_3/\partial a_1 & \partial x_3/\partial a_2 & \partial x_3/\partial a_3 \end{bmatrix} \quad (5)$$

These results will be used for the interpretation of the deformation matrices $\partial x_i/\partial a_j$ used later for calculations.

Calculated Results

The present section will present calculated results showing the effects of contraction on the acoustic energy produced. Two types of calculations will be performed. First, a calculation is performed for a realistic model using the deformation tensor calculated for a specific aerodynamic case using the method in Part 1. Following this, calculations are performed for assumed deformation tensors; this allows investigation into the effect of varying a specific parameter of the contraction tensor on the noise.

The acoustic calculations performed here use an effective radius rather than performing the integration over rotor span in order to shorten calculation time. This is an approximation that is often used in rotor calculations. The results are expected to follow essentially the same behavior as would be obtained by integrating over the rotor span.

Previous publications[3,13,23] have given results for the case of an isotropic turbulence input. Reference 23 gives several fundamental conclusions for the simplest case of hover in isotropic turbulence. These are repeated below for general background.

1) The acoustic energy has a V_t^4 dependence at low frequency and a V_t^3 dependence at high frequency where V_t is the rotor velocity. This change from a fourth to a third order dependence on velocity arises because of the change in the airfoil response function between low and high frequency. Dipole noise is generally assumed to have a fifth or sixth power dependence on the velocity, but this assumes that the turbulence-fluctuation intensity also depends on the velocity, whereas here the turbulence intensity is assumed to be fixed as the velocity V_t is increased.

2) The acoustic energy increases nearly linearly with blade number assuming that other blade parameters are kept fixed.

3) The effect of blade chord on the noise is small for wavelengths greater than about 4 chords. For chords small compared to the wavelength, the noise is proportional to the square of the chord.

4) The noise spectrum at a given frequency varies with the $-\frac{2}{3}$ power of the turbulence integral scale except when L is comparable to or less than the chord and the frequency is low.

5) The directivity plots tend to flatten toward the rotor plane somewhat when the Mach number is significant. This results from the tendency for sound to be directed forward from a moving sound source.

These results are generally what would be expected for an airfoil in rectilinear motion through the turbulent field. Recall that the present model calculates the noise by assuming a series of rectilinear motions as the airfoil moves around the azimuth.

The first calculation presented below is for the case of a helicopter in what is termed "pseudohover." The term pseudohover is used since it was necessary to assume a nonzero mean flow at infinity; otherwise the contraction ratio for an eddy originating far from the rotor would be infinite since the ratio of mean velocities far from the rotor and near the rotor would be infinite. Thus, the calculated contraction ratio must, of course, depend on the forward-flight velocity. For a low-flight velocity, the contraction will approach infinity, whereas for a high-flight velocity, the contraction will approach 1. The parameters used for calculating the distortion tensor are given in Ref. 20. They are horizontal freestream velocity = 2.57 m/s, rotor advance ratio = 0.014, rotor induced velocity = 7.68 m/s, and wake skew angle = 18.5 deg. The atmospheric parameters are Z = helicopter height = 122 m, L = Morin-Obukhov length = ∞, G = geostrophic wind speed = 5.1 m/s; these are defined in Part 1 of this paper.

The mean-flow distortion program, described in Part 1, can be used to calculate the deformation matrix at any point on the rotor face. Two points are chosen here for acoustic calculations. Both lie on a line parallel to the mean flow at infinity and passing through the rotor hub. The first is at 95% of the rotor radius near the leading part of the rotor disk. The second point at which the deformation matrix is calculated is at 95% of the rotor radius near the trailing part of the rotor disk.

Case A: Point Near the Leading Part of the Rotor Disk

The deformation matrix near the leading part of the rotor disk and in the plane of the disk was found to be

$$\partial a_i/\partial x_j = \begin{bmatrix} 1.39 & 0.00 & 0.00 \\ 0.00 & -0.06 & -0.65 \\ 0.00 & 1.38 & 2.81 \end{bmatrix} \quad (6a)$$

The inverse of this matrix is

$$\partial x_i/\partial a_j = \begin{bmatrix} 0.719 & 0.00 & 0.00 \\ 0.00 & 4.115 & -1.918 \\ 0.00 & 0.904 & -0.083 \end{bmatrix} \quad (6b)$$

Equations (6a) and (6b) can be used to find ϵ_{ij} and η_{ij}, respectively, as given by Eqs. (2) and (3). This gives

$$\epsilon_{ij} = \begin{bmatrix} -4.66 & 0 & 0 \\ 0 & 0.287 & 1.003 \\ 0 & 1.003 & -4.83 \end{bmatrix} \quad (7a)$$

$$\eta_{ij} = \begin{bmatrix} -2.42 & 0 & 0 \\ 0 & 9.81 & 1.94 \\ 0 & 1.94 & -0.0879 \end{bmatrix} \quad (7b)$$

The three principal values of the ϵ_{ij} matrix are

$$P_1 = -0.466$$
$$P_2 = 0.477$$
$$P_3 = -5.023$$

The three principal values of the η_{ij} matrix are

$$Q_1 = -0.242$$
$$Q_2 = 10.17$$
$$Q_3 = -0.454$$

The deformations in the three principal directions are then found using Eqs. (4a) or (4b) to be

$$(ds/ds_0)_1 = 0.719$$
$$(ds/ds_0)_2 = 4.62$$
$$(ds/ds_0)_3 = 0.302$$

The first of these, $(ds/ds_0)_1$, represents the contraction in the rotor plane and transverse to the mean flow at infinity. The second and third represent distortions in the plane normal to the line of the first distortion. The second represents a stretching by a factor of 4.62. In principle, one would have to calcu-

late the angle of the principal axes and the amount of rotation to find the angle of these last two deformations. Because of the rather large deformation, however, one can assume that this principal strain direction will lie close to the streamlines. For this case, the axial Mach number is 0.033, and the vertical Mach number is 0.016. Thus, the flow is at an angle of 25 deg from the rotor plane, and the strain ellipsoid would be expected to be aligned approximately along the same direction.

Case B: Point Near the Trailing Edge of the Rotor Disk

The deformation matrix near the trailing part of the rotor disk for the same flight parameters as case A was found to be

$$\partial a_i/\partial x_j = \begin{bmatrix} 4.63 & 0.00 & 0.00 \\ 0.00 & 6.29 & -2.41 \\ 0.00 & 0.61 & -0.21 \end{bmatrix} \tag{8a}$$

with the inverse

$$\partial x_i/\partial a_j = \begin{bmatrix} 0.216 & 0.00 & 0.00 \\ 0.00 & -1.41 & 16.15 \\ 0.00 & 4.09 & 42.16 \end{bmatrix} \tag{8b}$$

It will be noted that these last two matrices do not have a determinant of exactly 1; for incompressible flow, the determinant should be 1. Maintaining accuracy in the calculation of the deformation becomes more difficult as the deformation magnitude increases. Because of the large deformation for this case, the fact that the determinant is not unity should not affect the basic conclusion.

Calculating the principal strains as above for this case gives

$$Q_1 = -0.4767$$
$$Q_2 = 1028.00$$
$$Q_3 = -0.4892$$

The deformations in the three principal directions are then

$$(ds/ds_0)_1 = 0.216$$
$$(ds/ds_0)_2 = 45.35$$
$$(ds/ds_0)_3 = 0.147$$

One notes immediately the large value of the deformation.

Calculated Sound

The acoustic program requires the deformation matrix as input. The nonisotropic turbulence is then calculated using rapid distortion theory as described in Part 1. (A fuller description along with the computer program is available in Ref. 19.) This gives a simple method for testing the effects on the noise of changing the distortion tensor. The preceding two cases are presented first, followed by several cases for simple deformation matrices.

The sound produced by inputting into the acoustic program a unity deformation matrix (for the case of isotropic turbulence) and by inputting Eqs. (6a) and (8a) for the case of turbulence having undergone a contraction is shown in Figs. 3–5. The parameters needed as input by the program, in addi-

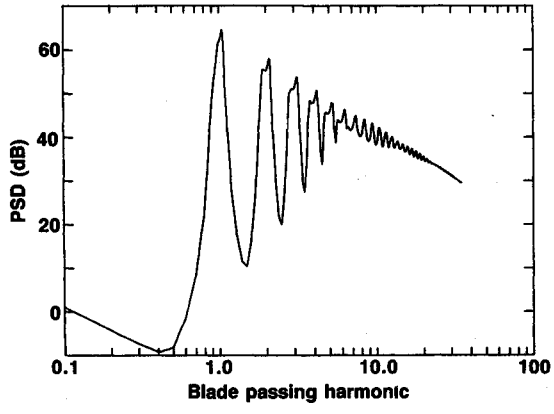

Fig. 3 Far-field power spectral density for distortion at point A on the rotor; distortion tensor given by Eq. (6a); $c_0 = 1410$, $B = 3$, $R_0/c = 15.8$, $r/c = 158$, rev/s = 7.5, $c/L = 0.005$, $M_z = 0.016$, $M_f = 0.033$, $\sqrt{w^2}/U_z = 0.048$.

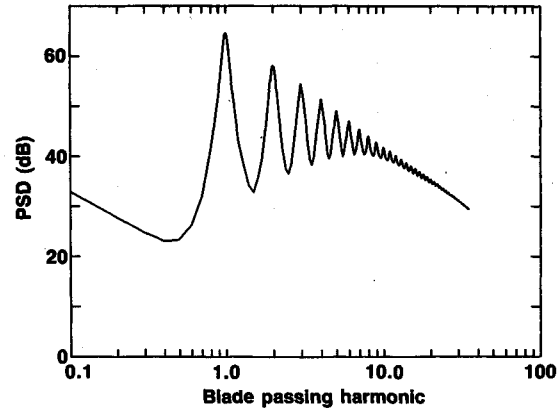

Fig. 4 Far-field PSD for isotropic distortion; same conditions as Fig. 3.

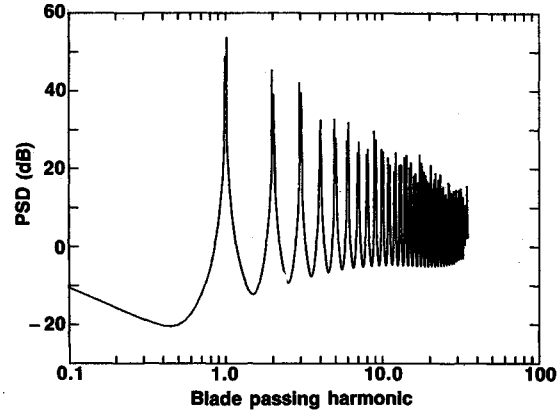

Fig. 5 Far-field PSD for distortion at point B on the rotor; distortion tensor given by Eq. (8a); $c_0 = 1410$, $B = 3$, $R_0/c = 15.8$, $r/c = 15^c$, rev/s = 7.5, $c/L = 0.005$, $M_z = 0.030$, $M_f = 0.011$, $\sqrt{w^2}/U_z = 0.025$.

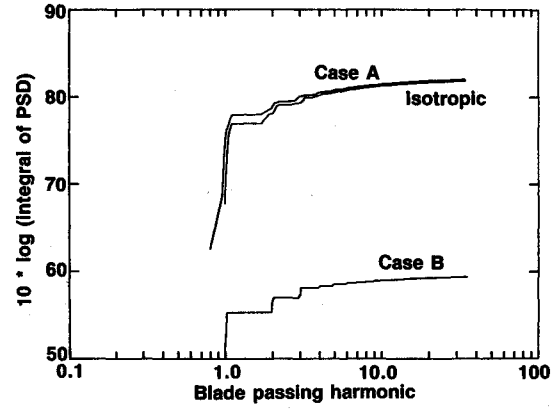

Fig. 6 Far-field acoustic energy for cases in Figs. 3–5.

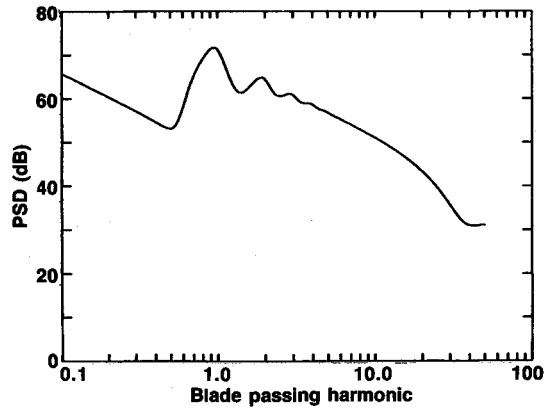

Fig. 7 Far-field PSD for axial compression $C=0.36$; $c_0=1000$, $B=3$, $R_0/c=10$, $r/c=100$, rev/s=10, $c/L=0.01$, $M_z=0.01$, $M_f=0$, $\sqrt{w^2}/U_z=0.01$.

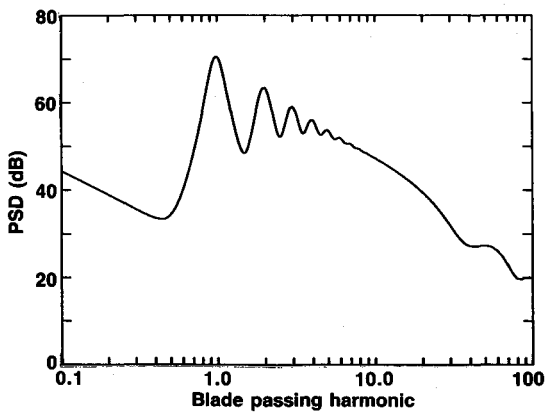

Fig. 8 Far-field PSD for isotropic turbulence; same conditions as Fig. 7.

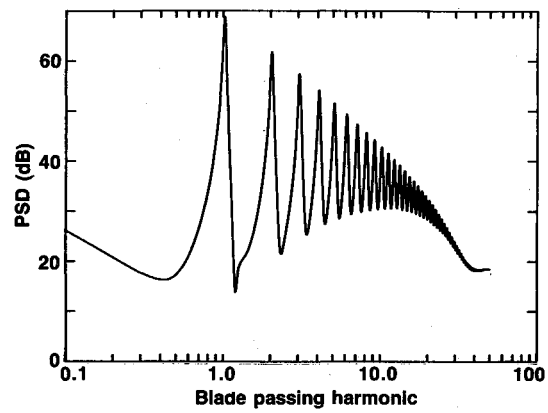

Fig. 9 Far-field PSD for axial contraction ratio $C=4$; same conditions as Fig. 7.

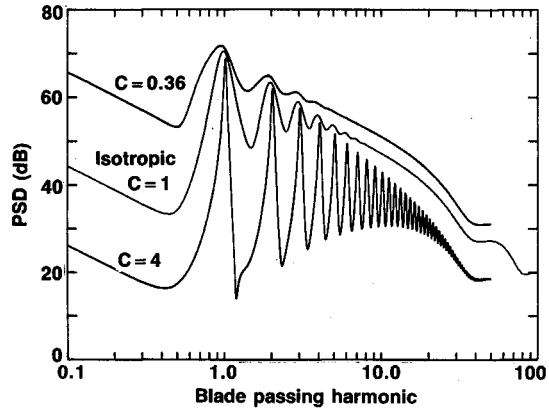

Fig. 10 Superposition of Figs. 7–9.

tion to the deformation matrix, are $M_t=0.529$, $c_0=1410$ ft/s, $B=3$, $R_0/c=15.8$, $r/c=158$, rev/s=7.5, and $c/L=0.005$ with the observer overhead of the rotor. These are assumed operating conditions. Additional parameters are calculated by the mean-flow contraction model and the atmospheric turbulence model described in Part 1. For the first deformation given by Eq. (6a) (case A), these additional parameters are $M_z=0.016$, $M_f=0.033$, and $\sqrt{w^2}/U_z=0.048$. These values are also used for the isotropic turbulence case. For the case given by Eq. (8a) (case B), these parameters are $M_z=0.030$, $M_f=0.011$, and $\sqrt{w^2}/U_z=0.025$.

The acoustic energy integrated over frequency is shown in Fig. 6. This figure shows the integrated energy between zero and the frequency on the abscissa. The figure shows a step-like behavior since the energy is concentrated in the harmonic peaks with little energy between. This shows that the contraction does little to change the acoustic energy between case A and the isotropic case. As shown in Fig. 2, the energy of the velocity perturbations in the direction of the stretching deformation is decreased, whereas the energy of the velocity perturbations in the other two directions is increased. At the small pitch for this case, the rotor blades lie nearly in the rotor plane. Since the deformation is at a rather substantial angle [the streamlines are at an angle of $\tan^{-1}(M_z/M_f)=\tan^{-1}(0.033/0.016)=64$ deg from the rotor axis], the rotor sees certain upwash velocities (normal to the blade) being increased and others being decreased from the isotropic turbulence case. The overall effect is rather small even though the contraction is 10.17, as given above. The pressure spectra also show little difference between the isotropic case (Fig. 3) and the nonisotropic case (Fig. 4). The most significant difference is that the minima in the spectra between peaks are lower for the isotropic case.

Case B, however, shows significant differences from the isotropic case. This case has a greater contraction (45.35), and it is at a smaller angle to the rotor axis [$\tan^{-1}(M_z/M_f)=\tan^{-1}(0.011/0.03)=20$ deg]. Thus, the velocities that are increased by the contraction have less of a contribution to the upwash, and those that are attenuated have a greater contribution. This shows up in both the power spectral density (PSD) and the integrated energy. In Fig. 2, one notes that the energy of the axial velocities for the contraction case is significantly attenuated from that for the isotropic turbulence case. There is a factor of more than 20 dB between the energy of the two cases. The PSD peak levels in Fig. 5 do not show the same 20 dB difference from the isotropic case, but the significantly narrower width for the nonisotropic case accounts for the energy difference. It is interesting to refer to Fig. 2 to try to confirm the magnitude of this effect. This shows that for a contraction of 10, the energy in the axial velocity is reduced by somewhat more than a factor of 10. For the contraction 45.35, the energy in the axial velocity is reduced by a factor of 4.31×10^{-3}; this is found from the analytical results in Ref. 18. This by itself gives a factor of 24 dB, which shows that a 20 dB effect with this contraction is quite reasonable.

The preceding two comparisons show that both the total amount of distortion and the direction of the distortion are important. This is illustrated further in the examples calculated below. The results are generally what one would expect. A stretching along the axis tends to decrease the noise since the velocities parallel to the stretching direction are attenuated; these are the velocities that are normal to the airfoil and produce the noise. If a given stretching along the axis of the rotor is then tilted so that the stretching lies at an angle, the noise begins to increase and in fact can be greater than the noise for the isotropic case if the angle is large enough. These principles are illustrated further below.

Effect of Axial Distortion

Figures 7–9 illustrate the effect of increasing the distortion along the axis. Three cases are given: Fig. 7 shows the case of a compression along the axis, a unit length of fluid in the axial direction being compressed to a length of 0.36, Fig. 8 shows the result for an isotropic turbulence, and Fig. 9 shows an axial extension of 4. The input parameters were rather arbitrarily chosen to be $c_0 = 1000$ ft/s, $B = 3$, $R_0/c = 10$, $r/c = 100$, rev/s = 10, $c/L = 0.01$, $M_z = 0.1$, $M_f = 0$, and $\sqrt{w^2}/U_z = 0.01$ with the observer overhead of the rotor.

Comparing Figs. 7 and 8, one notes that the levels for the contraction case are slightly higher than those for the isotropic turbulence case. Also, the peaks are significantly wider in frequency. This is as one would expect since for a compression along the axis, there will be much less of a tendency for multiple eddy chopping and, therefore, a broadening of the peaks. Also, the axial velocities (the upwash velocities) will generally be increased, whereas the velocities in the rotor plane will be attenuated. Finally, because the eddies have an increased length scale in the rotor plane due to the eddy stretching in the rotor plane, one might expect a higher sound amplitude at low frequency. This is seen to be the case.

The same comments can be made on comparing Figs. 8 and 9; only now the isotropic case produces more noise. Figure 9, for an axial stretching by a factor of 4, shows a narrowing of the harmonic peaks because of the greater tendency for multiple eddy chopping. The low subharmonic frequencies are attenuated because of the diminished length scales produced by the stretching. It is interesting that the peak amplitudes for the three cases are nearly the same. Only the width and the depth of the trough between peaks changes significantly. This is illustrated in Fig. 10 where the three figures are superimposed.

The energy integrated over frequency for these three cases is shown in Figs. 11 and 12. Figure 11 shows the energy integral as a function of frequency, and Figure 12 shows the overall acoustic energy vs contraction. Figure 12 shows a fairly linear relation between the log of the integrated energy and the log of the contraction ratio. Reference 18 shows that the axial energy behaves as C^{-2}, where C is the contraction ratio. In fact, the slope of Fig. 12 is slightly less than that for an inverse square. This difference could be attributed to other factors such as the change in the correlation length due to the contraction.

Effect of Strain Tensor Rotation

The effect of rotation of the principal strain direction from the vertical can be found by rotating the strain matrix using the rotation matrix

$$N = \begin{bmatrix} 1 & 0 & 0 \\ 0 & \cos\alpha & \sin\alpha \\ 0 & -\sin\alpha & \cos\alpha \end{bmatrix}$$

The strain matrix n'_{ij} after rotation of the axes by the angle α is related to the strain matrix η_{ij} before the rotation by

$$\eta'_{ij} = N^T \eta_{ij} N \tag{9}$$

where the T on N denotes the transpose.

Figures 9, 13, and 14 show the effect of rotating the strain tensor on the noise. The mean parameters are the same as for the preceding case. As one might expect, rotation of the strain ellipsoid away from the axis of the rotor and toward the plane of the rotor gives an increase in the noise. Also, the spectra show increasing width of the peaks as the principal axis rotates into the plane of the rotor. This is as one would expect since there will be fewer blade intersections of a given eddy when the short axis of the eddy is oriented in the flow direction.

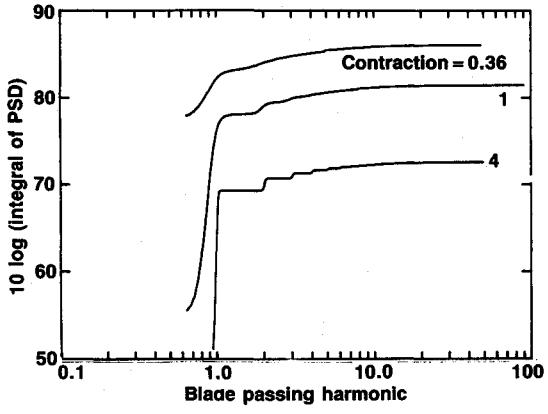

Fig. 11 Acoustic energies of Figs. 7–9.

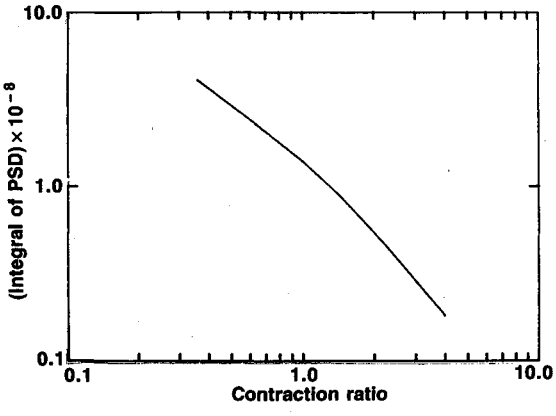

Fig. 12 Acoustic energy vs contraction ratio; same conditions as Fig. 7.

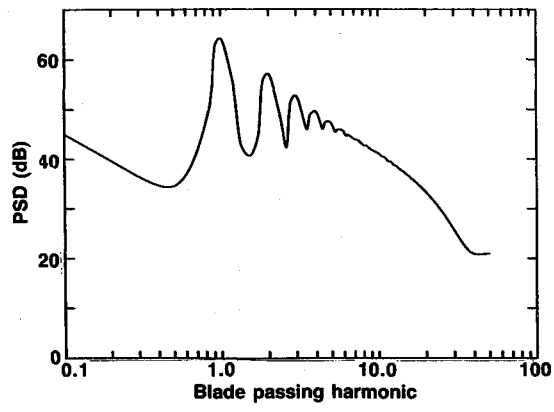

Fig. 13 Far-field PSD for contraction ratio $C = 4$, rotated to 45 deg; same conditions as Fig. 7.

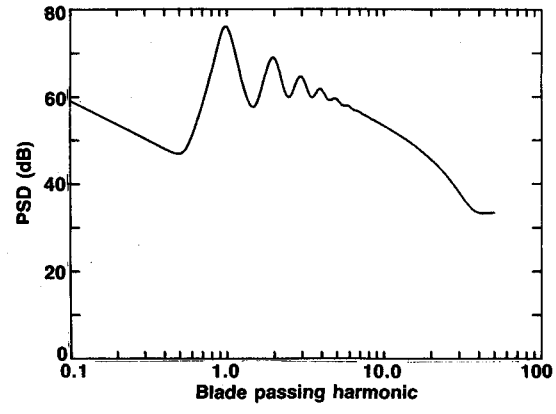

Fig. 14 Far-field PSD for contraction ratio $C = 4$, rotated to 90 deg rotor plane; same conditions as Fig. 7.

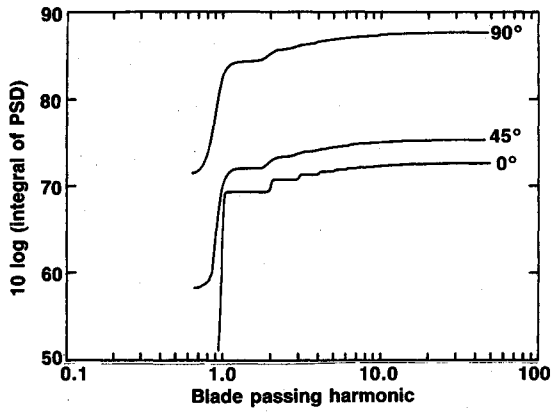

Fig. 15 Acoustic energies of Figs. 9, 13, and 14.

The overall energy is plotted in Fig. 15, and one notes that there is only a change of a few dB in energy in going from 0–45 deg of rotation, but much more change in going from 45–90 deg. One possible explanation of this concerns the correlation area seen by the blade. If one considers the area of intersection of a very long eddy with the blade, one notes that the area is proportional to $1/\cos\alpha$, where α is the angle of tilt away from the axis. Thus, when α approaches 90 deg, the correlation area becomes infinite. Of course, the eddy is not infinite, but for eddies that are stretched significantly, the correlation area increases rapidly as the angle approaches 90 deg. In addition, the axial turbulence velocities increase as θ approaches 90 deg, which further increases the noise.

Figure 15 can also be compared with the result for isotropic turbulence in Fig. 11. This shows that both the cases of stretched turbulence at 0 deg and at 45 deg produce less energy than the isotropic turbulence case. The result for 90 deg (the principal strain lying in the rotor plane) gives a greater noise than the isotropic turbulence case by approximately 5 dB. It appears that the distortion of turbulence generally leads to a decrease of the noise when compared to the isotropic case, but it is possible to achieve an increased noise if the principal axis of the distortion tensor lies close to the rotor axis. This will generally occur only if the velocity of forward flight is somewhat greater than the axial flow through the rotor. Thus, case A in Fig. 6 gives slightly greater noise than the isotropic case. The principal strain direction is also at a very large angle (approximately 64 deg) with the rotor axis, and the deformation shows a stretching of nearly a factor of five. Increasing the forward-flight velocity further than a certain level, however, will lead to less strain; thus, even though the principal strain direction may approach closer to the rotor plane, the noise will not be increased further. Also, as the forward-flight velocity is increased, for a realistic calculation, the rotor plane would be tilted forward, rotating the principal strain direction back toward the rotor axis and decreasing the noise.

Conclusions

Several significant conclusions can be drawn from the preceding calculations regarding the effects of turbulence distortion on the noise generation as it interacts with a helicopter rotor. These conclusions confirm the results one would expect from the consideration of a simple axial distortion and its effects on the energy of the velocity fluctuations in the three coordinate directions.

1) A simple distortion along the axis of the rotor gives a decrease in the acoustic energy and a decrease in the width of the harmonic peaks. This decrease is due mainly to the attenuation of the axial perturbation velocities and can be very significant. Also, the narrowband random peaks extend to higher frequency for an axial stretching of the turbulence. Conversely, a compression of the turbulence along the axis gives an increase in the acoustic energy.

2) For a given stretching of the turbulence, the noise increases as the principal axis of stretching is rotated toward the rotor plane; also, the width of the peaks is increased. This variation with angle is strongest when the principal axis is near the rotor plane. The variation with angle for angles of the stretching near the rotor axis is relatively weak. If the angle of stretching lies near the rotor plane, the acoustic energy can be greater than that for the nondistorted isotropic turbulence.

3) Caution should be used in drawing conclusions about noise generation based only on the amplitude of a harmonic peak without consideration of the peak width. The energy in a peak is generally more important than peak amplitude alone, and the peak width can vary significantly with the distortion, affecting the energy.

Acknowledgments

The authors would like to thank NASA Langley Research Center for supporting this research (Contract NAS1-17096) and Tom Brooks for acting as contract monitor.

References

[1]Simonich, J. C., Amiet, R. K., Schlinker, R. S., and Greitzer, E. M., "Rotor Noise Due to Atmospheric Turbulence Ingestion, Part I—Fluid Mechanics," *Journal of Aircraft,* Vol. 27, Jan. 1990, pp. 7–14.

[2]Hanson, D. B., "Measurements of Static Inlet Turbulence," AIAA Paper 75-467, 1975.

[3]Paterson, R. W. and Amiet, R. K., "Noise of a Model Helicopter Rotor due to Ingestion of Isotropic Turbulence," *Journal of Sound and Vibration,* Vol. 85, No. 4, Dec. 1982, pp. 551–577.

[4]George, A. R., "Helicopter Noise: State of the Art," *Journal of Aircraft,* Vol. 15, Nov. 1978, pp. 707–715.

[5]Brooks, T. F. and Schlinker, R. H., "Progress in Rotor Broadband Noise Research," *Vertica,* Vol. 7, No. 4, 1983, pp. 287–307.

[6]Sharland, I. F., "Sources of Noise in Axial Flow Fans," *Journal of Sound and Vibration,* Vol. 1, 1964, pp. 302–322.

[7]Dean, L. W., "Broadband Noise Generated by Airfoils in Turbulent Flow," AIAA Paper 71-587, 1971.

[8]Mugridge, B. D., "Sound Radiation from Airfoils in Turbulent Flow," *Journal of Sound and Vibration,* Vol. 13, No. 3, Nov. 1970, pp. 362–363.

[9]Mani, R., "Noise Due to Interaction of Inlet Turbulence with Isolated Stators and Rotors," *Journal of Sound and Vibration,* Vol. 17, No. 2, 1971, pp. 251–260.

[10]Amiet, R. K., "Acoustic Radiation from an Airfoil in a Turbulent Stream," *Journal of Sound and Vibration,* Vol. 41, No. 4, 1975, pp. 407–420.

[11]Paterson, R. W. and Amiet, R. K., "Acoustic Radiation and Surface Pressure Characteristics of an Airfoil Due to Incident Turbulence," NASA CR-2733, 1976.

[12]Homicz, G. F. and George, A. R., "Broadband and Discrete Frequency Radiation from Subsonic Rotors," *Journal of Sound and Vibration,* Vol. 36, No. 2, Sept. 1974, pp. 151–17.

[13]Amiet, R. K., "Noise Produced by Turbulent Flow into a Propeller or Helicopter Rotor," *AIAA Journal,* Vol. 15, March 1977, pp. 307–308.

[14]George, A. R. and Chow, S. J., "Broadband Rotor Noise Analyses," NASA CR-3797, 1984.

[15]George, A. R. and Kim, Y. N., "High Frequency Broadband Rotor Noise," *AIAA Journal,* Vol. 15, April 1977, pp. 538–545.

[16]Lowson, M. V., "The Sound Field for Singularities in Motion," *Proceedings of the Royal Society,* London, Vol. A286, 1965, pp. 559–572.

[17]Ribner, H. S. and Tucker, M., "Spectrum of Turbulence in a Contracting Stream," NACA TR-1113, 1953.

[18]Batchelor, G. K. and Proudman, I., "The Effect of Rapid Distortion of a Fluid in Turbulent Motion," *Quarterly Journal of Mechanics and Applied Mathematics,* Vol. 7, 1954, pp. 83–103.

[19]Amiet, R. K., "The Spectrum of Turbulence Undergoing a Rapid Distortion," United Technologies Research Center, East Hartford, CT, Rept. UTRC84-26, 1984.

[20]Simonich, J. C., Amiet, R. K., Schlinker, R. S., and Greitzer, E. M., "Helicopter Rotor Noise due to Ingestion of Atmospheric Turbulence," NASA CR-3973, 1986.

[21]Love, A. E. H., *A Treatise on the Mathematical Theory of Elasticity,* Dover, New York, 1927, pp. 62–64.

[22]Pearson, C. E., *Theoretical Elasticity,* Harvard University Press, Cambridge, MA, 1959, pp. 69–70.

[23]Amiet, R. K., "Noise Due to Rotor Turbulence Interaction," NASA Helicopter Acoustics, CP-2052, 1978, pp. 109–126.